An excursion into Nonsmooth Dynamics: from Mechanics, to Electronics, through Control

Vincent Acary

An excursion into Nonsmooth Dynamics: from Mechanics, to Electronics, through Control

Vincent Acary

INRIA Rhône–Alpes, Grenoble.
vincent.acary@inrialpes.fr

Fifty Years of Finite Freedom Mechanics.
On the occasion of Michel Jean's 70$^{\text{th}}$ birthday
Marseille, 25–27 October 2010

Contents

Mechanical systems with contact, impact and friction

From the mechanics of divided Materials. . .

Mechanical systems with contact, impact and friction

Stack of beads with perturbation

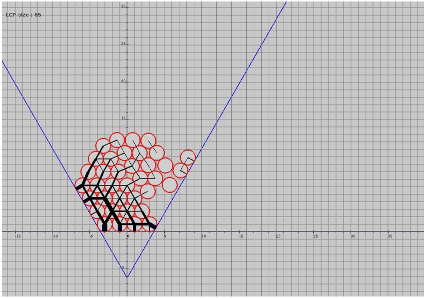

Mechanical systems with contact, impact and friction

Mechanical systems with contact, impact and friction

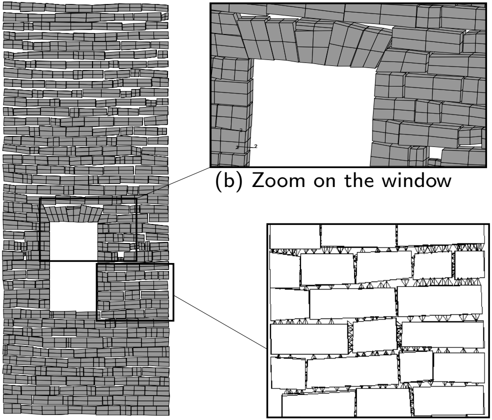

(a) FEM H8 meshing

(b) Zoom on the window

(c) Contact detection

Mechanical systems with contact, impact and friction

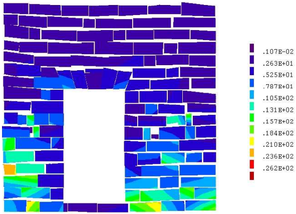

Figure: von Mises stresses

Mechanical systems with contact, impact and friction

Divided Materials and Masonry

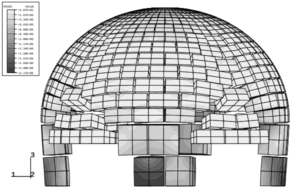

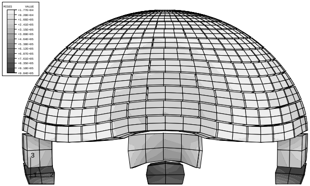

Mechanical systems with contact, impact and friction

FEM models with contact, friction cohesion, etc...

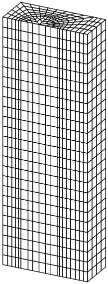

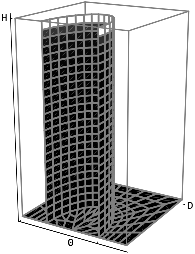

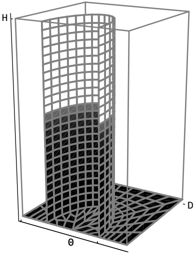

Joint work with Y. Monerie, IRSN.

Mechanical systems with contact, impact and friction

to the dynamics of Multibody and robotic systems . . .

Mechanical systems with contact, impact and friction

Simulation of Circuit breakers (INRIA/Schneider Electric)

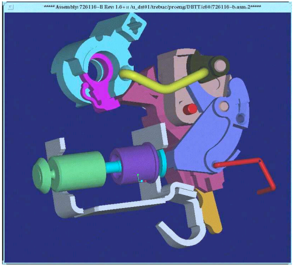

Mechanical systems with contact, impact and friction

Bipedal Robot INRIA BIPOP

Mechanical systems with contact, impact and friction

Towards controlled robotic systems on granular materials

Mechanical systems with contact, impact and friction

Simulation of the ExoMars Rover (INRIA/Trasys Space/ESA)

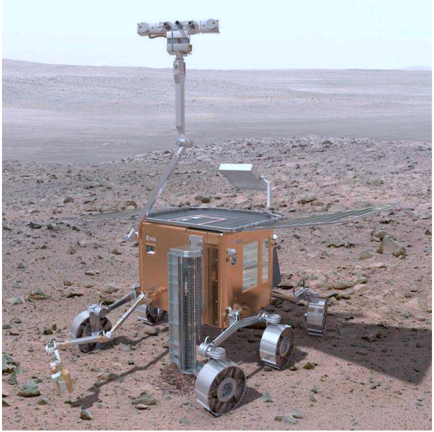

Mechanical systems with contact, impact and friction

They are all nonsmooth mechanical systems but they differ in

- the presence of perfect nonlinear joints,
- the presence of finite rotations,
- the presence of Control (sensors & actuators)
- the desired properties in design and development which influence the numerical simulation and prototyping

Unilateral constraints as an inclusion

Definition (Perfect unilateral constraints on the smooth dynamics)

$$\begin{cases} M(q)\dfrac{dv}{dt} + F(t,q,v) = r \\ \\ -r \in N_{\mathcal{C}(t)}(q(t)) \end{cases} \tag{1}$$

where

- $r = \nabla_q g(q,t)\,\lambda$ is the generalized reactions due to the constraints.
- Finite set of ν unilateral constraints on the generalized coordinates :

$$g(q,t) = [g_\alpha(q,t) \geqslant 0, \quad \alpha \in \{1 \dots \nu\}]^T. \tag{2}$$

- Admissible set $\mathcal{C}(t)$

$$\mathcal{C}(t) = \{q \in \mathcal{M}(t), g_\alpha(q,t) \geqslant 0, \alpha \in \{1 \dots \nu\}\}. \tag{3}$$

- Normal Cone to $\mathcal{C}(t)$

$$N_{\mathcal{C}(t)}(q(t)) = \left\{ \begin{array}{r} y \in \mathbb{R}^n \mid y = -\sum_\alpha \lambda_\alpha \nabla g_\alpha(q,t), \\ \lambda_\alpha \geqslant 0,\ \lambda_\alpha g_\alpha(q,t) = 0 \end{array} \right\} \tag{4}$$

Non Smooth Lagrangian Dynamics

Fundamental assumptions.

- The velocity $v = \dot{q}$ is of Bounded Variations (B.V)
  ➜ The equation are written in terms of a right continuous B.V. (R.C.B.V.) function, v^+ such that

$$v^+ = \dot{q}^+ \tag{5}$$

- q is related to this velocity by

$$q(t) = q(t_0) + \int_{t_0}^{t} v^+(t)\, dt \tag{6}$$

- The acceleration, ($\ddot{q}$ in the usual sense) is hence a differential measure dv associated with v such that

$$dv(]a,b]) = \int_{]a,b]} dv = v^+(b) - v^+(a) \tag{7}$$

Non Smooth Lagrangian Dynamics

Definition (Non Smooth Lagrangian Dynamics)

$$\begin{cases} M(q)dv + F(t, q, v^+)dt = di \\ \\ v^+ = \dot{q}^+ \end{cases} \tag{8}$$

where di is the reaction measure and dt is the Lebesgue measure.

Remarks

- The non smooth Dynamics contains the impact equations and the smooth evolution in a single equation.
- The formulation allows one to take into account very complex behaviors, especially, finite accumulation (Zeno-state).
- This formulation is sound from a mathematical Analysis point of view.

References

[Schatzman, 1973, 1978, Moreau, 1983, 1988]

Non Smooth Lagrangian Dynamics

Decomposition of measure

$$\left\{ \begin{array}{rrrr} dv = & \gamma\, dt + & (v^+ - v^-)\, d\nu + & dv_s \\ di = & f\, dt + & p\, d\nu + & di_s \end{array} \right. \tag{9}$$

where

- $\gamma = \ddot{q}$ is the acceleration defined in the usual sense.
- f is the Lebesgue measurable force,
- $v^+ - v^-$ is the difference between the right continuous and the left continuous functions associated with the B.V. function $v = \dot{q}$,
- $d\nu$ is a purely atomic measure concentrated at the time t_i of discontinuities of v, i.e. where $(v^+ - v^-) \neq 0$,i.e. $d\nu = \sum_i \delta_{t_i}$
- p is the purely atomic impact percussions such that $pd\nu = \sum_i p_i \delta_{t_i}$
- dv_S and di_S are singular measures with the respect to $dt + d\eta$.

Impact equations and Smooth Lagrangian dynamics

Substituting the decomposition of measures into the non smooth Lagrangian Dynamics, one obtains

Definition (Impact equations)

$$M(q)(v^+ - v^-)d\nu = p d\nu, \tag{10}$$

or

$$M(q(t_i))(v^+(t_i) - v^-(t_i)) = p_i, \tag{11}$$

Definition (Smooth Dynamics between impacts)

$$M(q)\gamma dt + F(t,q,v)dt = f dt \tag{12}$$

or

$$M(q)\gamma^+ + F(t,q,v^+) \quad = \quad f^+ \quad [dt - a.e.] \tag{13}$$

The Moreau's sweeping process of second order

Definition (Moreau [1983, 1988])

A key stone of this formulation is the inclusion in terms of velocity. Indeed, the inclusion (1) is "replaced" by the following inclusion

$$\begin{cases} M(q)dv + F(t,q,v^+)dt = di \\ \\ v^+ = \dot{q}^+ \\ \\ -di \in N_{T_C(q)}(v^+) \end{cases} \tag{14}$$

Comments

This formulation provides a common framework for the non smooth dynamics containing inelastic impacts without decomposition.

➜ Foundation for the time–stepping approaches.

The Moreau's sweeping process of second order

Comments

- *The inclusion concerns measures.* Therefore, it is necessary to define what is the inclusion of a measure into a cone.
- *The inclusion in terms of velocity* v^+ rather than of the coordinates q.

Interpretation

- Inclusion of measure, $-di \in K$
  - Case $di = r'dt = fdt$.
$$-f \in K \tag{15}$$
  - Case $di = p_i \delta_i$.
$$-p_i \in K \tag{16}$$
- Inclusion in terms of the velocity. Viability Lemma
  If $q(t_0) \in C(t_0)$, then
$$v^+ \in T_C(q), t \geqslant t_0 \Rightarrow q(t) \in C(t), t \geqslant t_0$$
  ➜ The unilateral constraints on q are satisfied. The equivalence needs at least an impact inelastic rule.

The Moreau's sweeping process of second order

The Newton-Moreau impact rule

$$-\, di \in N_{T_{C}(q(t))}(v^{+}(t) + e v^{-}(t)) \tag{17}$$

where e is a coefficient of restitution.

Velocity level formulation. Index reduction

$$\begin{array}{ccc} -\lambda \in N_{\mathbb{R}^+}(y) & \rightsquigarrow & -\lambda \in N_{T_{\mathbb{R}^+}}(\dot{y}) \\ & \Updownarrow & \\ 0 \leqslant y \perp \lambda \geqslant 0 & \rightsquigarrow & \text{if } y \leqslant 0 \text{ then } 0 \leqslant \dot{y} \perp \lambda \geqslant 0 \end{array} \tag{18}$$

State–of–the–art

Numerical time–integration methods for Nonsmooth Multibody systems (NSMBS):

Nonsmooth event capturing methods (Time–stepping methods)

- $\oplus$ robust, stable and proof of convergence
- $\oplus$ low kinematic level for the constraints
- $\oplus$ able to deal with finite accumulation
- $\ominus$ very low order of accuracy even in free flight motions

Nonsmooth event tracking methods (Event–driven methods)

- $\oplus$ high level integration of free flight motions
- $\ominus$ no proof of convergence
- $\ominus$ sensibility to numerical thresholds
- $\ominus$ reformulation of constraints at higher kinematic levels.
- $\ominus$ unable to deal with finite accumulation

Objectives & means

Objectives

Design nonsmooth event capturing methods with

- same properties as standard methods (robustness, accumulation, . . .)
- Higher resolution (ratio error/computational cost)
- Higher order of accuracy

Means

1. Adaptive time–step size and order strategies for standard methods
2. Mixed integrators with rough pre-detection of events
3. Splitting strategies
4. Ad hoc detection of discontinuity and order of discontinuity methods.

NonSmooth Multibody Systems (NSMBS)

Academic examples

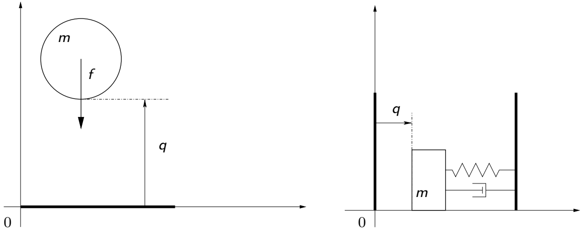

(a) Bouncing ball example (b) Linear Oscillator example

Figure: Academic test examples with analytical solutions

NonSmooth Multibody Systems (NSMBS)

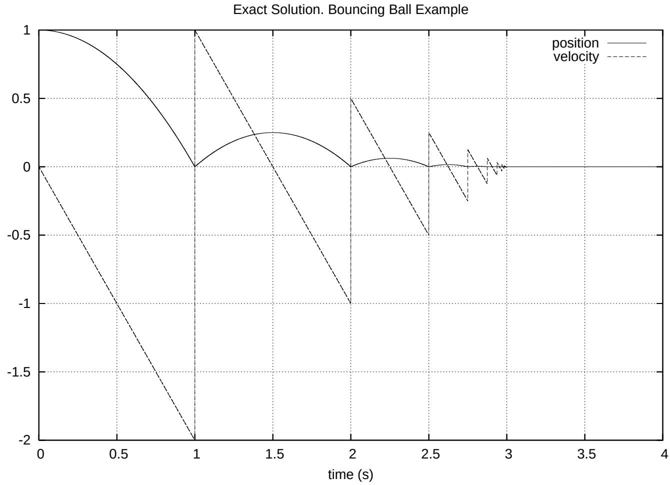

Figure: Analytical solutions. Bouncing ball example]

NonSmooth Multibody Systems (NSMBS)

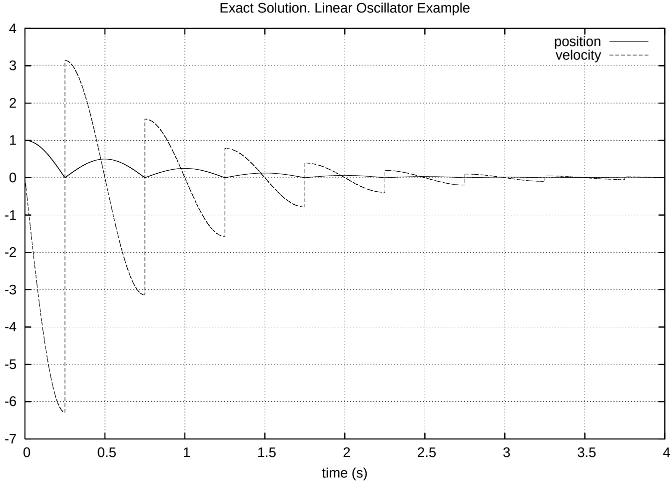

Figure: Analytical solutions. Linear Oscillator

Moreau–Jean's Time stepping scheme [Moreau, 1988] and [Jean, 1999]

Principle of NSCD

$$
\begin{cases}
M(q_{k+\theta})(v_{k+1} - v_k) - h\tilde{F}_{k+\theta} = G(q_{k+\theta})P_{k+1}, & \text{(19a)} \\
q_{k+1} = q_k + hv_{k+\theta}, & \text{(19b)} \\
U_{k+1} = G^T(q_{k+\theta})\, v_{k+1} & \text{(19c)} \\
-P_{k+1} \in N_{T_{\mathbb{R}^m_+}(\tilde{y}_{k+\gamma})}(U_{k+1} + eU_k), & \text{(19d)} \\
\tilde{y}_{k+\gamma} = y_k + h\gamma U_k, \quad \gamma \in [0,1]. & \text{(19e)}
\end{cases}
$$

with $\theta \in [0,1], \gamma \geqslant 0$ and $x_{k+\alpha} = (1-\alpha)x_{k+1} + \alpha x_k$ and $\tilde{y}_{k+\gamma}$ is a prediction of the constraints.

Schatzman's Time stepping scheme [Paoli and Schatzman, 2002]

Principle

$$
\begin{cases}
M(q_k+1)(q_{k+1}-2q_k+q_{k-1}) - h^2 F(t_{k+\theta}, q_{k+\theta}, v_{k+\theta}) = p_{k+1}, & \text{(20a)} \\
v_{k+1} = \dfrac{q_{k+1}-q_{k-1}}{2h}, & \text{(20b)} \\
-p_{k+1} \in N_K\left(\dfrac{q_{k+1}+eq_{k-1}}{1+e}\right), & \text{(20c)}
\end{cases}
$$

where N_K defined the normal cone to K.
For $K = \{q \in \mathbb{R}^n, y = g(q) \geqslant 0\}$

$$
0 \leqslant g\left(\frac{q_{k+1}+eq_{k-1}}{1+e}\right) \perp \nabla g\left(\frac{q_{k+1}+eq_{k-1}}{1+e}\right) P_{k+1} \geqslant 0 \qquad (21)
$$

Comparison

Shared mathematical properties

- Convergence results for one constraints
- Convergence results for multiple constraints problems with acute kinetic angles
- No theoretical proof of order

Mechanical properties

- Position vs. velocity constraints
- Respect of the impact in one step (Moreau–Jean) vs. Two-steps(Schatzman)
- Linearized constraints rather than nonlinear.

Empirical order of convergence. Moreau–Jean's time–stepping scheme

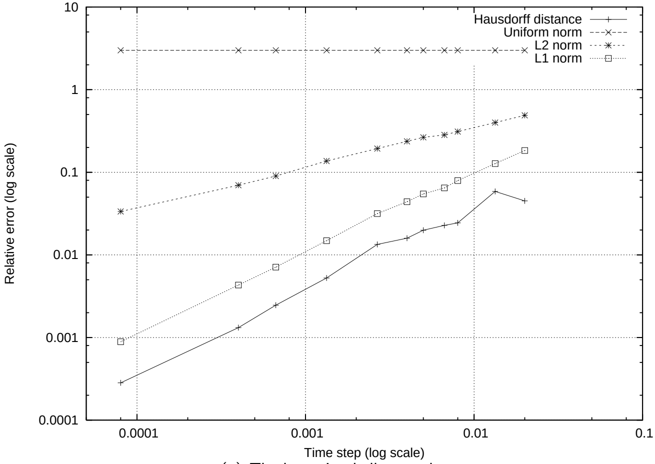

(a) The bouncing ball example

Figure: Empirical order of convergence of the Moreau–Jean's time-stepping scheme.

Empirical order of convergence. Moreau–Jean's time–stepping scheme

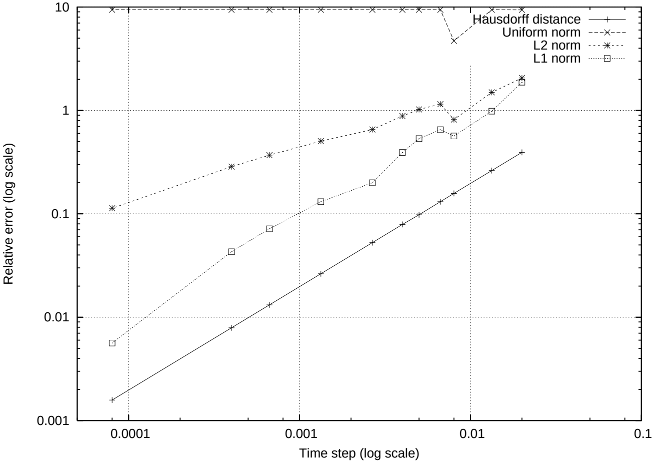

(a) The linear oscillator example

Figure: Empirical order of convergence of the Moreau–Jean's time-stepping scheme.

Empirical order of convergence. Schatzman–Paoli's time–stepping scheme

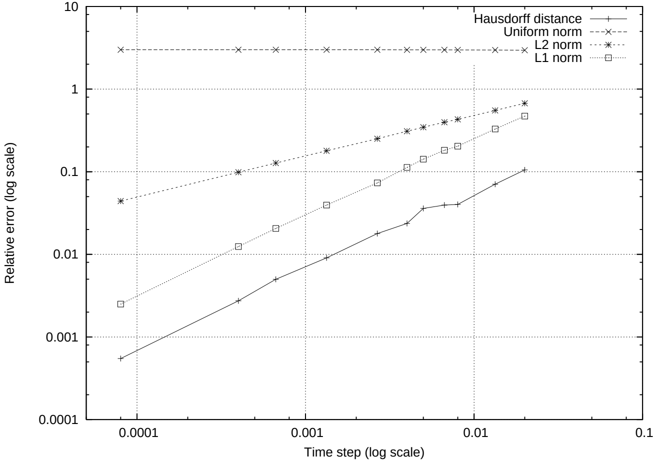

(a) The bouncing ball example

Figure: Empirical order of convergence of the Schatzman-Paoli's time-stepping scheme.

Empirical order of convergence. Schatzman–Paoli's time–stepping scheme

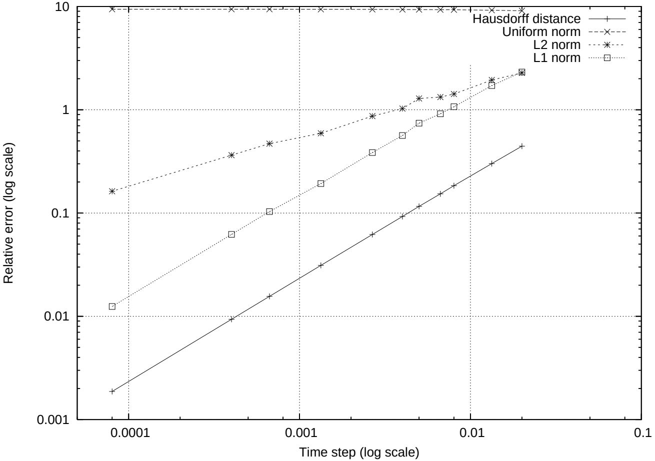

(a) The linear oscillator example

Figure: Empirical order of convergence of the Schatzman-Paoli's time-stepping scheme.

Local error estimates for the Moreau-Jean's time–stepping

Assumption 1 : Existence and uniqueness

A unique global solution over $[0, T]$ for Moreau's sweeping process is assumed such that $q(\cdot)$ is absolutely continuous and admits a right velocity $v^+(\cdot)$ at every instant t of $[0, T]$ and such that the function $v^+ \in LBV([0, T], \mathbb{R}^n)$.

➜ Assumption 1 is ensured in the framework introduced by Ballard [Ballard, 2000] who proves the existence and uniqueness of a solution in a general framework mainly based on the analyticity of data.

Assumption 2 : Smoothness of data

The following smoothness on the data will be assumed: a) the inertia operator $M(q)$ is assumed to be of class $\mathcal{C}^p$ and definite positive, b) the force mapping $F(t, q, v)$ is assumed to be of class $\mathcal{C}^p$, c) the constraint functions $g(q)$ are assumed to be of class $\mathcal{C}^{p+1}$ and d) the Jacobian matrix $G(q) = \nabla_q^T g(q)$ is assumed to have full-row rank.

Local error estimates for the Moreau-Jean's time–stepping

Lemma

Let $I = [t_k, t_{k+1}]$. Let us assume that the function $f \in BV(I, \mathbb{R}^n)$. Then we have the following inequality for the θ–method, $\theta \in [0, 1]$,

$$\left\| \int_{t_k}^{t_{k+1}} f(s)\,ds - h(\theta f(t_{k+1}) + (1-\theta) f(t_k)) \right\| \leqslant C(\theta)(t_{k+1} - t_k)\, var(f, I), \tag{22}$$

where $var(f, I) \in \mathbb{R}$ is the variation of f on I and $C(\theta) = \theta$ if $\theta \geqslant 1/2$ and $C(\theta) = 1 - \theta$ otherwise. Furthermore, the value of $C(\theta)$ yields a sharp bound in (22).

Local error estimates for the Moreau-Jean's time–stepping

Proposition

Under Assumptions 1 and 2, the local order of consistency of the Moreau-Jean time–stepping scheme for the generalized coordinates is

$$e_q = q_{k+1} - q(t+h) = \mathcal{O}(h)$$

and at least for the velocities

$$e_v = v^+(t_k + h) - v_{k+1} = \mathcal{O}(1)$$

.

Comments

The bounds are reached if an impact is located within the time–step and the activation of the constraint is not correct.

Higher Order Time–stepping schemes

Background

Work of Mannshardt [1978] on time–integration schemes of any order for ODE/DAEs with discontinuities (with tranversality assumption)

Principle

- Let us assume only one event per time–step at instants t_*.
- Choose any ODE/DAE solvers of order p
- Perform a rough location of the event inside the time step of length h
  Find an interval $[t_a, t_b]$ such that

$$t_* \in [t_a, t_b] \text{ and } |t_b - t_a| = Ch^{p+1} + \mathcal{O}(h^{p+2}) \tag{23}$$

  Dichotomy, Newton, Local Interpolants, Dense output,...
- Perform an integration on $[t_k, t_a]$ with the ODE solver of order p
- Perform an integration on $[t_a, t_b]$ with Moreau's time–stepping scheme
- Perform an integration on $[t_b, t_{k+1}]$ with the ODE solver of order p

Integration of the smooth dynamics

Mainly for the sake of simplicity, the numerical integration over a smooth period is made with a Runge–Kutta (RK) method on the following index-1 DAE,

$$\begin{cases} M(q(t))\dot{v}(t) = F(t,q(t),v(t)) + G(q)\lambda(t), \\ \dot{q}(t) = v(t), \\ \gamma(t) = G(q(t))\dot{v}(t) = 0. \end{cases} \tag{24}$$

In practice, the time–integration is performed for the following system

$$\begin{cases} M(q(t))\dot{v}(t) = F(t,q(t),v(t)) + G(q)\lambda(t), \\ \dot{q}(t) = v(t), \\ 0 \leqslant \gamma(t) = G(q(t))\dot{v}(t) \perp \lambda(t) \geqslant 0 \end{cases} \tag{25}$$

on the time–interval I where the index set $\mathcal{I}(t)$ of active constraints is assumed to be constant on I and $\lambda(t) > 0$ for all $t \in I$.

Integration of the smooth dynamics

Using the standard notation for the RK methods (see Hairer et al. [1993] for details), the complementarity problem that we have to solve at each time–step reads

$$\begin{cases} t_{ki} = t_k + c_i h, \\ v_{k+1} = v_k + h \sum_{i=1}^{s} b_i V'_{ki}, \\ q_{k+1} = q_k + h \sum_{i=1}^{s} b_i V_{ki}, \\ V'_{ki} = M^{-1}(Q_{ki}) \left[F(t_{ki}, Q_{ki}, V_{ki}) + G(Q_{ki}) \lambda_{ki} \right], \\ V_{ki} = v_k + h \sum_{j=1}^{s} a_{ij} V'_{nj}, \\ Q_{ki} = q_k + h \sum_{j=1}^{s} a_{ij} V_{nj}, \\ 0 \leqslant \gamma_{ki} = G(Q_{ki}) V'_{ki} \perp \lambda_{ki} \geqslant 0. \end{cases} \tag{26}$$

Assumption 3

Let I a smooth period time–interval. We assume that

1. the local order of the RK method (26) is p that is

$$e_q = e_v = \mathcal{O}(h^{p+1}) \tag{27}$$

2. starting from inconsistent initial value $\tilde{q}_k$ such that $\tilde{q}_k - q_k = \mathcal{O}(h^{p+1})$, the error made by the RK method (26) is

$$\tilde{q}_{k+1} - q_{k+1} = \mathcal{O}(h^{p+1}) \tag{28}$$

Theorem

Let us assume that Assumptions 1, 2 and 3 hold. The local error of consistency of the scheme is of order p in the generalized coordinates that is

$$e_q = \mathcal{O}(h^{p+1}). \tag{29}$$

Results on the linear oscillator

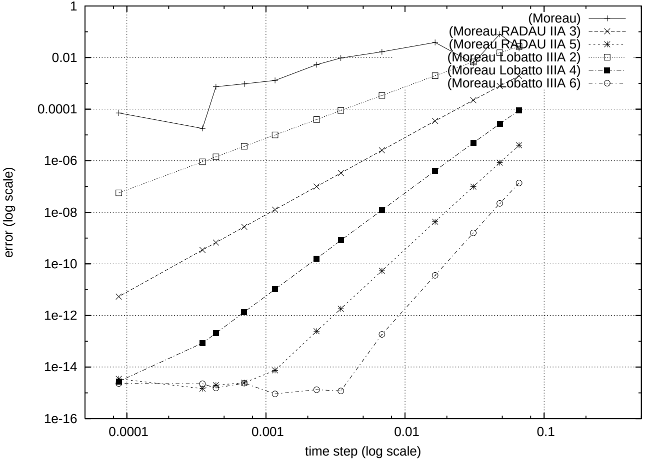

(a) The linear oscillator example with implicit Runge Kutta Method

Figure: Precision Work diagram for the Moreau's time-stepping scheme coupled with Runge–Kutta method.

Finite accumulation

- Repeat the whole process on the remaining part of the interval $[t_b, t_k]$
- By induction, repeat this process up to the end of the original time step.

Results on the Bouncing Ball

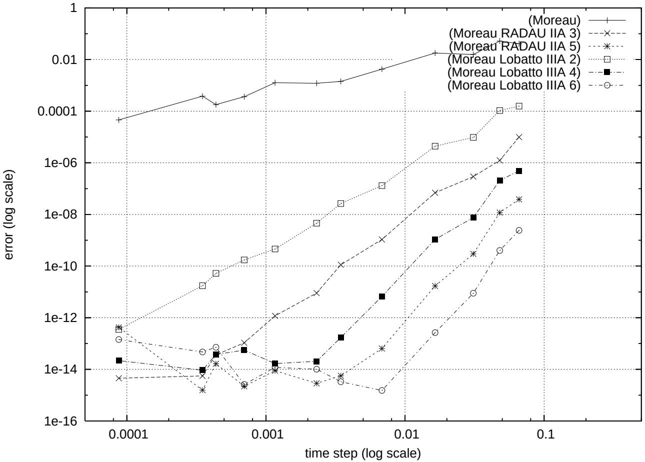

(a) The Bouncing Ball example with implicit Runge Kutta Method

Figure: Precision Work diagram for the Moreau's time-stepping scheme.

Contents

Sliding Mode Control for dummies

Basic principles on a naive example

Problem: Stabilization of this simple dynamics

$$\begin{cases} x(t_0) = x_0 \in \mathbb{R} \\ \dot{x} = f, \quad |f| \leqslant 1, \end{cases} \tag{30}$$

at the origin $x = 0$.

Naive solution:

$$\begin{cases} x(t_0) = x_0 \in \mathbb{R} \\ \dot{x} = f + u, \quad |f| < 1, \end{cases} \tag{31}$$

- "Push on right" if the state is at the right of 0

$$u = -1 \text{ if } x > 0 \tag{32}$$

- "Push on right" if the state is at the left of 0

$$u = +1 \text{ if } x > 0 \tag{33}$$

- "balance the external load" in 0

$$u = -f \text{ if } x = 0 \tag{34}$$

Sliding Mode Control for dummies

Basic principles on a naive example

- Switched control based on the sign function

$$u = -\mathrm{sign}(x) = \begin{cases} -1 \text{ for } x > 0 \\ +1 \text{ for } x < 0 \\ ? \text{ for } x = 0 \end{cases} \tag{35}$$

  Definition of u at $x = 0$?

- Discontinuous ODEs

$$\dot{x} = f - \mathrm{sign}(x) \tag{36}$$

  Notion of solutions ?

Mathematical framework

- Multivalued maximal monotone operator

$$u = -\mathrm{sgn}(x) = \begin{cases} -1 \text{ for } x > 0 \\ +1 \text{ for } x < 0 \\ [-1, 1] \text{ for } x = 0 \end{cases} \tag{37}$$

- Filippov's differential inclusions

In the continuous setting

- Robust control w.r.t external uncertainties
- Finite time convergence to target

➜ SMC is the most widely used non linear control in industrial practice.

In the discrete setting

Digital implementation of SMC suffers from "chattering" due to explicit approximation

$$x_{k+1} - x_k = f - \mathrm{sgn}(x_k) \tag{38}$$

This causes

- Wear and damage in actuators
- Need for complex filtering systems which entails the good properties of continuous SMC.

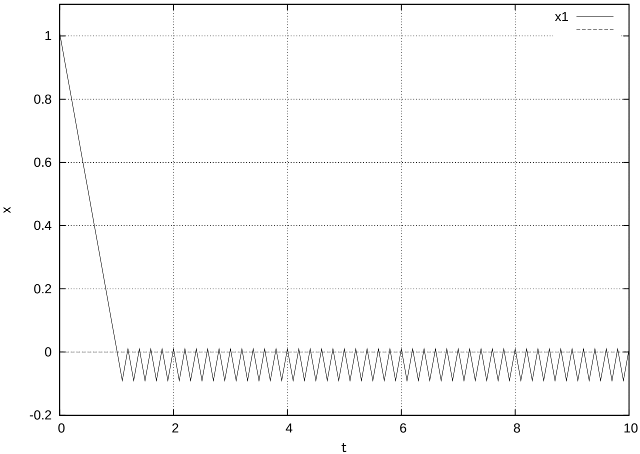

(a) $h = 0.2$

Figure: A simple example for $x_0 = 1.01$ at $t_0 = 0$.

Implicit Implementation of SMC

Our background

- Nonsmooth modelling of Friction
- Well–posedness analysis of Monotone Differential Inclusions
- Implicit numerical time integration for DI.

Objectives

- Study the implicit Euler discretization of a class of differential inclusions with sliding surfaces ($\subset$ Filippov's systems)
- Show that this numerical method permits a smooth stabilization on the sliding surface, in a finite number of steps
- Show how this may be used in real-time implementations of sliding mode control

To start with we consider the simplest case:

$$\dot{x}(t) \in -\mathrm{sgn}(x(t)) = \begin{cases} 1 & \text{if} \quad x(t) < 0 \\ -1 & \text{if} \quad x(t) > 0 \\ \text{[-1,1]} & \text{if} \quad x(t) = 0 \end{cases}, \quad x(0) = x_0 \tag{39}$$

with $x(t) \in \mathbb{R}$. This system possesses a unique Lipschitz continuous solution for any x_0. The backward Euler discretization of (39) reads as:

$$\begin{cases} x_{k+1} - x_k = -h s_{k+1} \\ s_{k+1} \in \mathrm{sgn}(x_{k+1}) \end{cases} \tag{40}$$

As is known the *explicit* Euler discretization of such discontinuous systems yields spurious oscillations around the switching surface [Galias et al, IEEE TAC and CAS 2006, 2007, 2008].

$\rightsquigarrow$ this means that the derivative of the switching function while sliding occurs, is very badly estimated.

Both the explicit and the implicit methods converge (the approximated solution $x^N(\cdot)$ tends to the Filippov's solution as $h \to 0$).
However or the backward Euler method the following holds:

Lemma

For all $h > 0$ and $x_0 \in \mathbb{R}$, there exists k_0 such that $x_{k_0+n} = 0$ and $\dfrac{x_{k_0+n+1} - x_{k_0+n}}{h} = 0$ for all $n \geqslant 1$.

On this simple case this has the following graphical interpretation, as the intersection of two graphs:

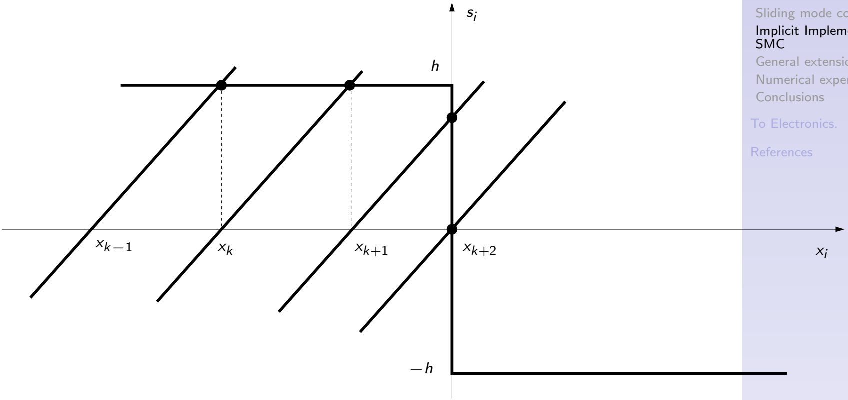

Figure: Iterations of the backward Euler method.

An interesting property is that the smooth stabilization and the finite-time convergence on the switching surface, hold (more or less) independently of the step $h > 0$:

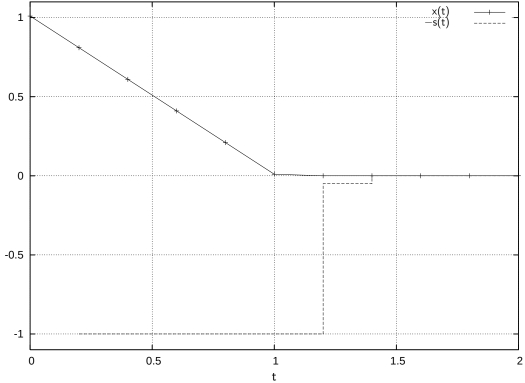

(a) $h = 0.2$

Figure: A simple example for $x_0 = 1.01$ at $t_0 = 0$.

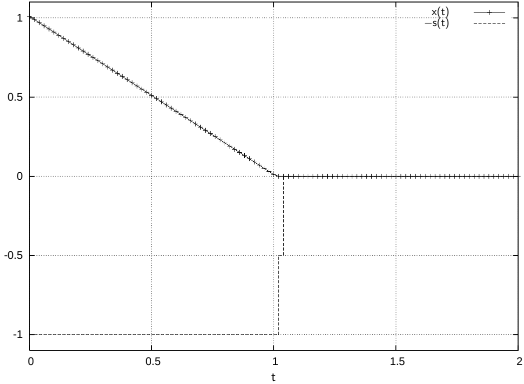

(a) $h = 0.02$

Figure: A simple example for $x_0 = 1.01$ at $t_0 = 0$.

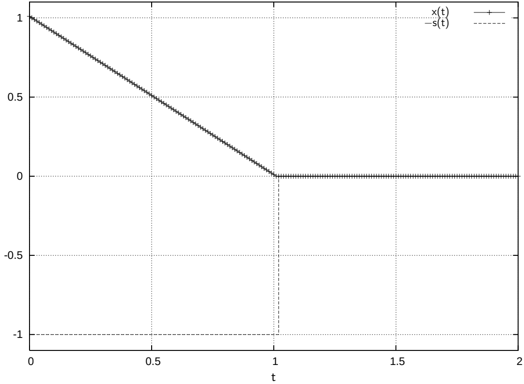

(a) $h = 0.01$

Figure: A simple example for $x_0 = 1.01$ at $t_0 = 0$.

General Extensions

We shall focus on inclusions of the form:

$$\begin{cases} \dot{x}(t) \in f(t, x(t)) - B\,\mathrm{Sgn}(Cx(t) + D), \;\text{ a.e. on } (0, T) \\ x(0) = x_0 \end{cases} \tag{41}$$

with

$B \in \mathbb{R}^{n\times m}$

$\mathrm{Sgn}(Cx(t) + D) \triangleq (\mathrm{sgn}(C_1 x + D_1), \ldots, \mathrm{sgn}(C_m x + D_m))^T \in \mathbb{R}^m$, where $sgn(\cdot)$ is multivalued at 0.

Well-posedness of the differential inclusions (41)

Proposition

Consider the differential inclusion in (41). Suppose that

- *There exists* $L \geqslant 0$ *such that for all* $t \in [0, T]$*, for all* $x_1, x_2 \in \mathbb{R}^n$*, one has* $||f(t, x_1) - f(t, x_2)|| \leqslant L||x_1 - x_2||$.
- *There exists a function* $\Phi(\,\cdot\,)$ *such that for all* $R \geqslant 0$*:*

$$\Phi(R) = \sup \left\{ \| \frac{\partial f}{\partial t}(\,\cdot\,, v) \|_{\mathcal{L}^2((0,T);\mathbb{R}^n)} \mid \| v \|_{\mathcal{L}^2((0,T);\mathbb{R}^n)} \leqslant R \right\} < +\infty.$$

If there exists an $n \times n$ *matrix* $P = P^T > 0$ *such that*

$$PB_{\bullet i} = C_{i\bullet}^T \tag{42}$$

for all $1 \leqslant i \leqslant m$*, then for any initial data the differential inclusion (41) has a unique solution* $x : (0, T) \rightarrow \mathbb{R}^n$ *that is Lipschitz continuous.*

Sketch of the proof

- Change of state variables $z = Rx$ where $R = R^T > 0$ and $R^2 = P$.
- Use a result in [Bastien-Schatzman ESAIM M2AN 2002] to conclude.

- The existence of a positive definite P such that $PB = C^T$ is satisfied in many instances of sliding-mode control: observer-based sliding-mode control, Lyapunov-based discontinuous robust control.
- This is an "input-output" constraint on the system, constraining the relative degree of the triple (A, B, C).
- It is satisfied when (A, B, C) is positive real (dissipative).

Time-discretization of (41)

The differential inclusion in (41) is therefore discretized as follows:

$$\begin{cases} \dfrac{x_{k+1} - x_k}{h} \in f(t_k, x_k) - B\mathrm{Sgn}(Cx_{k+1} + D), \ \text{a.e. on } (0, T) \\ x(0) = x_0 \end{cases} \tag{43}$$

From [Bastien-Schatzman ESAIM M2AN 2002] we have that:

Proposition

Under Proposition 2 conditions, there exists η such that for all $h > 0$ one has

$$\text{For all } t \in [0, T], \ ||x(t) - x^N(t)|| \leqslant \eta\sqrt{h} \tag{44}$$

Moreover
$\lim_{h\to 0^+} \max_{t\in[0,T]} ||x(t) - x^N(t)||^2 + \int_0^t ||x(s) - x^N(s)||^2 ds = 0.$

However we have more: the discrete state reaches the sliding surface (when it exists) in a finite number of steps, and stabilizes on it in a smooth way.

Let $y(t) \stackrel{\Delta}{=} Cx(t) + D$.

Lemma

Let us assume that a sliding mode occurs for the index $\alpha \subset \{1 \dots m\}$, *that is* $y_\alpha(t) = 0, t > t_*$. *Let* C *and* B *be such that (42) holds and* $C_{\alpha\bullet}B_{\bullet\alpha} > 0$. *Then there exists* $h_c > 0$ *such that* $\forall h < h_c$, *there exists* $k_0 \in \mathbb{N}$ *such that* $y_{k_0+n} = Cx_{k_0+n+1} + D = 0$ *for all integers* $n \geqslant 1$.

Such algorithms are similar to proximal algorithms which possess finite-time stabilization properties [Baji and Cabot, Set-Valued Analysis 2006].

Remarks

- Contrarily to other methods that reduce (not suppress...) chattering, the discrete-time sliding surface is equal to the continuous-time sliding surface.
- At each step one has to solve a generalized equation with unknown x_{k+1} that takes the form of a mixed linear complementarity system (MLCP).
- Specific MLCP solvers are needed to implement the method.

Numerical experiments

Let us consider the following two examples:

$$\dot{x} = \begin{bmatrix} 0 & 1 \\ 0 & -c_1 \end{bmatrix} x - \begin{bmatrix} 0 \\ \alpha \end{bmatrix} \mathrm{sgn}(\begin{bmatrix} c_1 & 1 \end{bmatrix} x). \tag{45}$$

(codimension one sliding surface)

$$B = \begin{bmatrix} 1 & 2 \\ 2 & -1 \end{bmatrix}, \quad C = \begin{bmatrix} 1 & 2 \\ 2 & -1 \end{bmatrix}, \quad D = 0, \quad f(x(t), t) = 0 \tag{46}$$

(codimension two sliding surface)

Numerical experiments

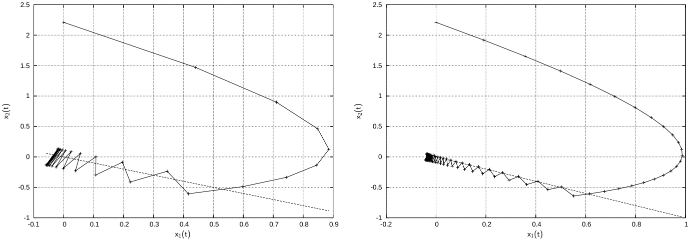

(a) $h = 0.3$. Explicit Euler

(b) $h = 0.1$. Explicit Euler

Figure: Equivalent control based SMC, $c_1 = 1, \alpha = 1$ and $x_0 = [0, 2.21]^T$. State $x_1(t)$ versus $x_2(t)$.

Numerical experiments

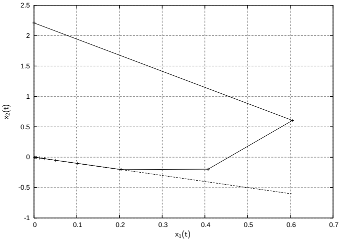

(a) $h = 1$. Implicit Euler

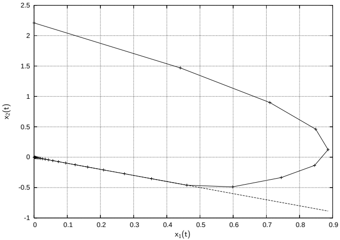

(b) $h = 0.3$. Implicit Euler

Figure: Equivalent control based SMC, $c_1 = 1, \alpha = 1$ and $x_0 = [0, 2.21]^T$. State $x_1(t)$ versus $x_2(t)$.

Numerical experiments

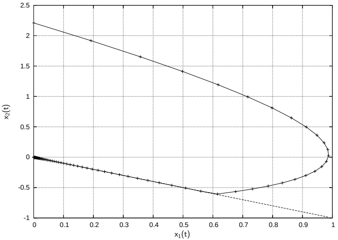

(a) $h = 0.1$. Implicit Euler

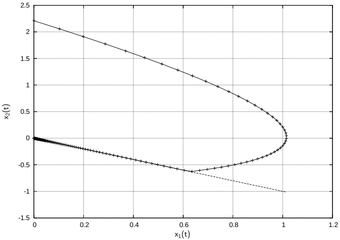

(b) $h = 0.05$. Implicit Euler

Figure: Equivalent control based SMC, $c_1 = 1, \alpha = 1$ and $x_0 = [0, 2.21]^T$. State $x_1(t)$ versus $x_2(t)$.

Numerical experiments

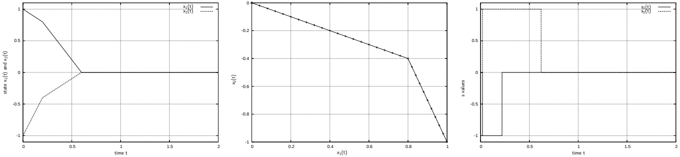

(a) state $x_1(t)$ and $x_2(t)$ versus time (b) phase portrait $x_2(t)$ versus $x_1(t)$ (c) sgn function $s_1(t)$ and $s_2(t)$

Figure: Multiple Sliding surface. $h = 0.02$, $x(0) = [1.0, -1.0]^T$

The system reaches firstly the sliding surface $2x_2 + x_1 = 0$ *without any chattering,* *The system then slides on the surface up to reaching the second sliding surface* $2x_1 - x_2 = 0$ *and comes to rest at the origin.*

The Filippov's example with switches accumulation

$$B = \begin{bmatrix} 1 & -2 \\ 2 & 1 \end{bmatrix}, \quad C = \begin{bmatrix} 1 & 0 \\ 0 & 1 \end{bmatrix}, \quad D = 0, \quad f(x(t), t) = 0. \quad (47)$$

The trajectories may slide on the codimension 2 surface given by $Cx = 0$. The origin is attained after an infinite number of switches in finite time.

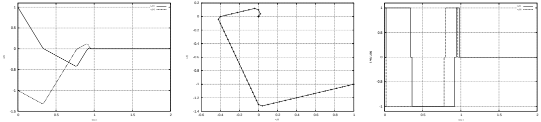

(a) state $x_1(t)$ and $x_2(t)$ versus time

(b) phase portrait $x_2(t)$ versus $x_1(t)$

(c) sgn function $s_1(t)$ and $s_2(t)$

Figure: Multiple Sliding surface. Filippov Example. $h = 0.002$, $x(0) = [1.0, -1.0]^T$

The results show that the system reaches the origin without any chattering.

Conclusions

The implicit Euler method allows one to nicely simulate the main features of sliding-mode systems:

- Finite-time stabilization on the switching surface (of codimension $\geqslant 1$)
- Smooth stabilization on the switching surface

It extends to the discrete-time implementation with ZOH discretization: looks like a promising solution for discrete-time sliding modes.

Contents

The RLC circuit with a diode

Example

A LC oscillator supplying a load resistor through a half-wave rectifier (see figure 14).

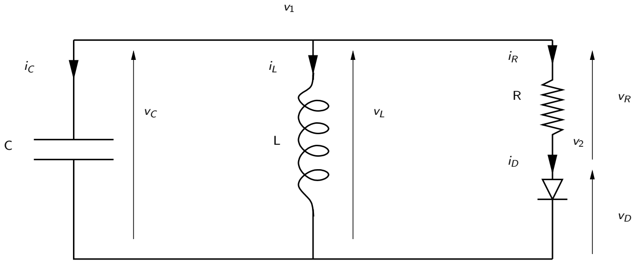

Figure: Electrical oscillator with half-wave rectifier

The RLC circuit with a diode

Example

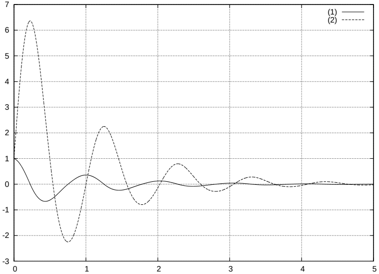

(a) state versus time v_L and i_L

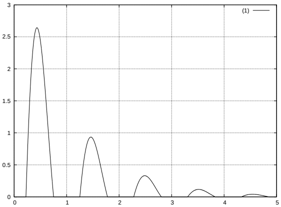

(b) Diode current i_D

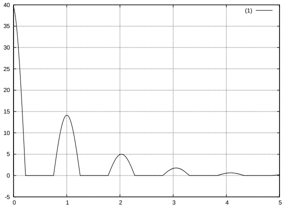

(c) Diode voltage v_D

The RLC circuit with a diode

Example

- Kirchhoff laws :

$$
\begin{array}{l}
v_L = v_C \\
v_R + v_D = v_C \\
i_C + i_L + i_R = 0 \\
i_R = i_D
\end{array}
$$

- Branch constitutive equations for linear devices are :

$$
\begin{array}{l}
i_C = C\dot{v}_C \\
v_L = L\dot{i}_L \\
v_R = Ri_R
\end{array}
$$

- "branch constitutive equation" of the diode

$$0 \in \mathcal{F}(i_D, V_D)$$

The RLC circuit with a diode

Example

The following dynamical system is obtained :

$$\begin{pmatrix} \dot{v}_L \\ \dot{i}_L \end{pmatrix} = \begin{pmatrix} 0 & \frac{-1}{C} \\ \frac{1}{L} & 0 \end{pmatrix} \cdot \begin{pmatrix} v_L \\ i_L \end{pmatrix} + \begin{pmatrix} \frac{-1}{C} \\ 0 \end{pmatrix} \cdot i_D$$

$$v_D = v_L - Ri_D$$

$$0 \in \mathcal{F}(v_D, i_D)$$

with the state variable $x \triangleq \begin{pmatrix} v_L \\ i_L \end{pmatrix}$ and $\lambda \triangleq i_D$, $y \triangleq v_D$, we get

$$\begin{cases} \dot{x} = Ax + B\lambda, \quad x \in \mathbb{R}^n, \lambda \in \mathbb{R}^m \\ y = Cx + D\lambda \\ 0 \in \mathcal{F}(y, \lambda) \end{cases} \tag{48}$$

Diode behavior

A modeling choice

smooth modeling | nonsmooth modeling

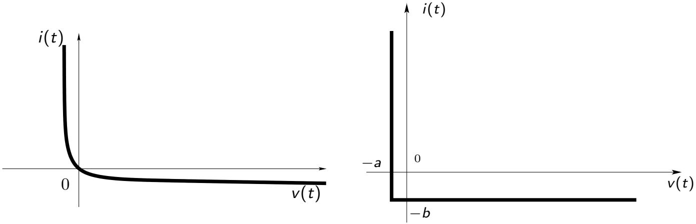

(a) $i(t) = i_s \exp(-\frac{v(t)}{\alpha} - 1)$

(b) $0 \leqslant i(t) + b \perp v(t) + a \geqslant 0$

Figure: Two models of diodes.

Diode behavior

Why a nonsmooth modeling ?

- To avoid stiff nonlinear models by using ideal constraints.
- To model the ideal behavior of switched components without artificial regularization

The diode–bridge rectifier

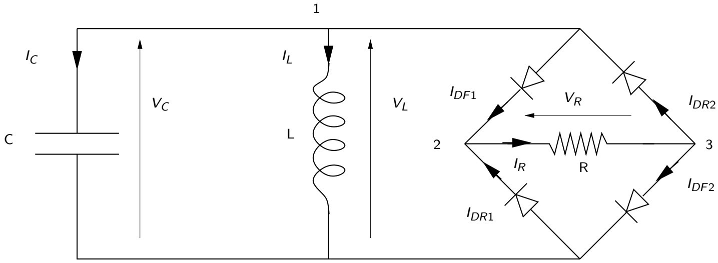

Figure: The Diode-bridge rectifier

The diode–bridge rectifier

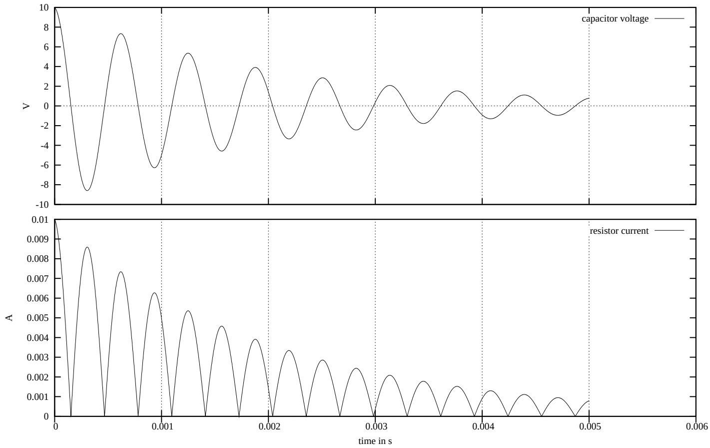

Figure: The Diode-bridge rectifier. Standard results

The diode–bridge rectifier

Differential systems

The dynamical equations are formulated as

$$\begin{cases} \dot{x} = Ax + B\lambda, \quad x \in \mathbb{R}^n, \lambda \in \mathbb{R}^m \\ y = Cx + D\lambda \\ 0 \leqslant y \perp \lambda \geqslant 0 \end{cases} \tag{49}$$

choosing :

$$x = \begin{bmatrix} V_L \\ I_L \end{bmatrix}, \quad \text{and } y = \begin{bmatrix} I_{DR1} \\ I_{DF2} \\ V_2 - V_1 \\ V_1 - V_3 \end{bmatrix}, \quad \lambda = \begin{bmatrix} V_2 \\ -V_3 \\ I_{DF1} \\ I_{DR2} \end{bmatrix}, \tag{50}$$

and with

$$A = \begin{bmatrix} 0 & -1/C \\ 1/L & 0 \end{bmatrix}, \quad B = \begin{bmatrix} 0 & -1/C & 1/C & 0 \\ 0 & 0 & 0 & 0 \end{bmatrix}$$

$$C = \begin{bmatrix} 0 & 0 \\ 0 & 0 \\ -1 & 0 \\ 1 & 0 \end{bmatrix}, \quad D = \begin{bmatrix} 1/R & 1/R & -1 & 0 \\ 1/R & 1/R & 0 & -1 \\ 1 & 0 & 0 & 0 \\ 0 & 1 & 0 & 0 \end{bmatrix} \tag{51}$$

A typical example of nonsmooth systems

Linear Complementarity Systems (LCS)

$$\begin{cases} \dot{x} = Ax + B\lambda, \quad x \in \mathbb{R}^n, \lambda \in \mathbb{R}^m \\ y = Cx + D\lambda \\ 0 \leqslant y \perp \lambda \geqslant 0 \end{cases} \tag{52}$$

with $A \in \mathbb{R}^{n\times n}, B \in \mathbb{R}^{n\times m}$
$C \in \mathbb{R}^{m\times n}, D \in \mathbb{R}^{m\times m}$, for m constraints.

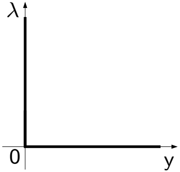

Piecewise linear systems

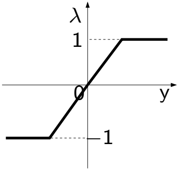

Saturation

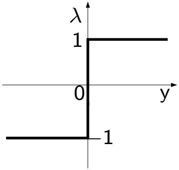

Relay

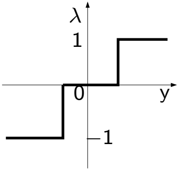

Relay with dead zone

A slightly more general class of nonsmooth systems

Differential inclusion into normal cones

$$\begin{cases} \dot{x} = Ax + B\lambda, \quad x \in \mathbb{R}^n, \lambda \in \mathbb{R}^m \\ y = Cx + D\lambda \\ -y \in N_K(\lambda) \end{cases} \tag{53}$$

where K is a convex set and $N_K(\lambda)$ stands for the normal cone to K taken at λ

Usual examples for K

- $K = \mathbb{R}^m$, then we obtain linear time invariant DAE

$$-y \in N_{\mathbb{R}^m}(\lambda) \Longleftrightarrow y = 0, \quad \lambda \in \mathbb{R}^m \tag{54}$$

- $K = \mathbb{R}^m_+$, then we obtain Linear Complementarity Systems (LCS)

$$-y \in N_{\mathbb{R}^m_+}(\lambda) \Longleftrightarrow 0 \leqslant y \perp \lambda \geqslant 0 \tag{55}$$

- $K = [-1, 1]^m$, then we obtain linear relay systems (related to Filippov's DI and sliding mode control).

$$-y \in N_{[-1,1]^m}(\lambda) \Longleftrightarrow \lambda \in \operatorname{sgn}(y) \tag{56}$$

Objectives

Our background

- Nonsmooth modeling of unilateral constraints and friction
- Nonsmooth analysis of dynamics with jumps.

Our Objectives

- Understand what can be the nature of the solutions (uniqueness, smoothness).
- How perform the numerical time–integration ?
- Open issues for the time–integration of large dynamical systems arising in electrical network applications.

Some results

Nature of solutions for $K \in \mathbb{R}^m_+$

The nature of solutions depends on

- the relative degree (index) between y and λ
- the possible consistency of the solution

The main types of solutions are

- $\mathcal{C}^1$ solutions when λ is a lipschitz function of x (relative degree 0)
- absolutely continuous solutions (relative degree 1)
- solutions of Bounded Variations (relative degree 2)

Some results

Numerical time–integration methods

The time integration methods depends on the solution

- $\mathcal{C}^1$ solutions : Standard DAE integrators of low order
- absolutely continuous solutions : Implicit first order scheme
- solutions of Bounded Variations : Moreau's catching up algorithm

Some results

Industrial circuits and automatic circuit equations formulation

- Adaptation of the standard Modified Nodal Analysis (MNA) to the nonsmooth elements to obtain

Problem (DGE)

$$\begin{array}{ll}
M(X,t)\dot{X} = D(X,t) + U(t) + R & \Big]\ \text{Differential Algebraic Equations} \\[2mm]
\begin{array}{l} y = G(X,\lambda,t) \\ R = H(X,\lambda,t) \end{array} & \left]\ \begin{array}{l}\text{Input/output relations} \\ \text{on nonsmooth components}\end{array}\right. \\[2mm]
0 \in F(y,\lambda,t) + T(y,\lambda,t) & \Big]\ \text{Generalized equation} \\[2mm]
X = [V, I_{\mathrm{L}}, I_{\mathrm{V}}, I_{\mathrm{NS}}]^T & \Big]\ \text{Variable definition}
\end{array} \tag{57}$$

➜ Difficulties to discuss the nature of solution and then to adapt the time numerical method

➜ In electrical circuits, the main difficulty is induced by the topology of the circuit rather than the inherent non–linearity of the components.

Applications to industrial electrical networks

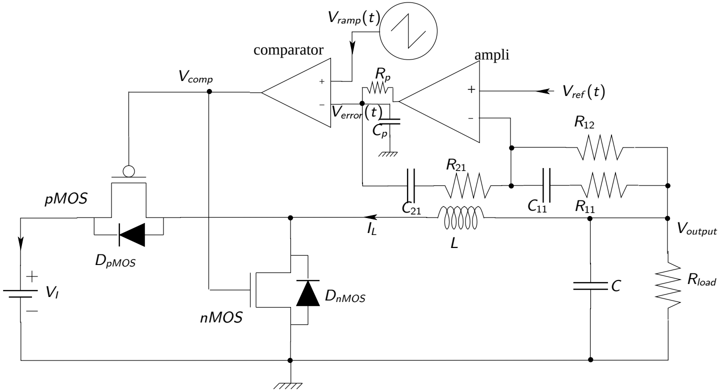

Figure: Buck converter.

Applications to industrial electrical networks

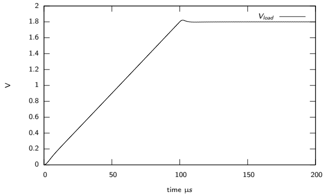

(a) V_{load}

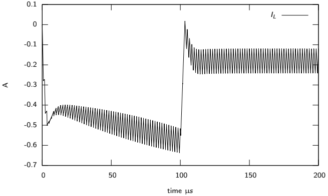

(b) I_L

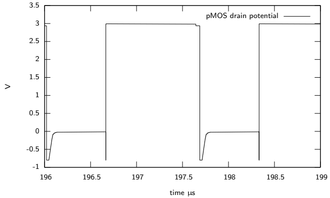

(c) pMOS drain potential

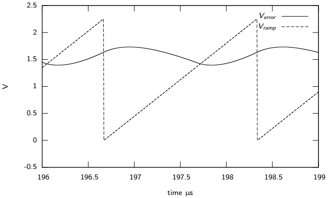

(d) V_{ramp} and V_{error}

Figure: SICONOS buck converter simulation using standard parameters.

Applications to industrial electrical networks

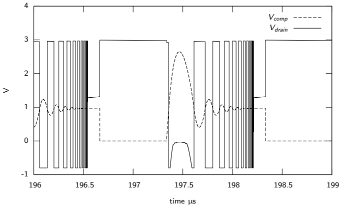

(a) V_{comp} and V_{drain}

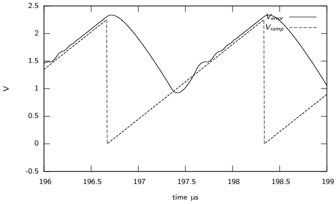

(b) V_{ramp} and V_{error}

Figure: SICONOS buck converter simulation using sliding mode parameters.

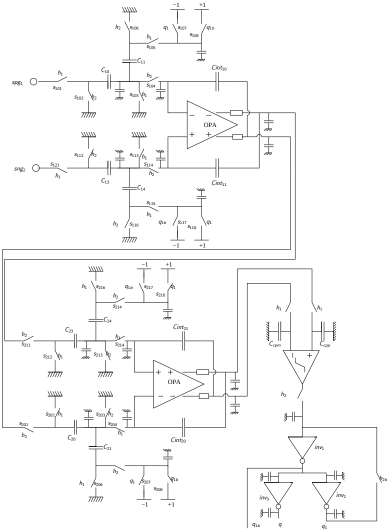

Figure: Delta-Sigma converter.

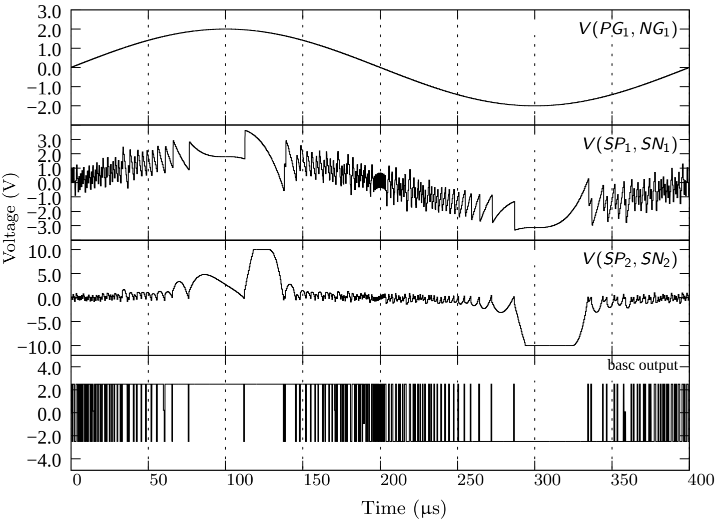

Figure: SICONOS simulation.

Open issues

For more general formulations and more complex systems, are we able to infer the nature of the solutions? That is to say,

- Define and predict an equivalent notion to index and relative degree for instance, for a matrix D semi-definite positive.
- Given passive components, are we able to forecast the nature of the solutions from some topological considerations ? (as for the DAE case.)
- Adapt the time–stepping schemes in an hierarchical way in taking into account the "index" of each variable.

and towards

- Dynamics of gene regulatory networks (cell physiology)
- . . .

Thank you for your attention.
Happy Birthday Michel and thank you again

P. Ballard. The dynamics of discrete mechanical systems with perfect unilateral constraints. *Archives for Rational Mechanics and Analysis*, 154:199–274, 2000.

E. Hairer, S.P. Norsett, and G. Wanner. *Solving Ordinary Differential Equations I. Nonstiff Problems.* Springer, 1993.

M. Jean. The non smooth contact dynamics method. *Computer Methods in Applied Mechanics and Engineering*, 177:235–257, 1999. Special issue on computational modeling of contact and friction, J.A.C. Martins and A. Klarbring, editors.

R. Mannshardt. One-step methods of any order for ordinary differential equations with discontinuous right-hand sides. *Numerische Mathematik*, 31:131–152, 1978.

J.J. Moreau. Liaisons unilatérales sans frottement et chocs inélastiques. *Comptes Rendus de l'Académie des Sciences*, 296 série II:1473–1476, 1983.

J.J. Moreau. Unilateral contact and dry friction in finite freedom dynamics. In J.J. Moreau and Panagiotopoulos P.D., editors, *Nonsmooth Mechanics and Applications*, number 302 in CISM, Courses and lectures, pages 1–82. CISM 302, Spinger Verlag, Wien- New York, 1988.

L. Paoli and M. Schatzman. A numerical scheme for impact problems I: The one-dimensional case. *SIAM Journal of Numerical Analysis*, 40(2): 702–733, 2002.

M. Schatzman. Sur une classe de problèmes hyperboliques non linéaires. *Comptes Rendus de l'Académie des Sciences Série A*, 1973.

M. Schatzman. A class of nonlinear differential equations of second order in time. *Nonlinear Analysis, T.M.A*, 2(3):355–373, 1978.